Inorg. Chem. **2006**, *45*, 4668−4676

Dinuclear Nickel and Palladium Complexes with Bridging 2,5-Diamino-1,4-benzoquinonediimines: Synthesis, Structures, and Catalytic Oligomerization of Ethylene

Jean-philippe Taquet, Olivier Siri, and Pierre Braunstein*

Laboratoire de Chimie de Coordination, UMR 7177 CNRS, Université Louis Pasteur, 4 rue Blaise Pascal, F-67070 Strasbourg Cedex, France

Richard Welter

Laboratoire DECOMET, UMR 7177 CNRS, Université Louis Pasteur, 4 rue Blaise Pascal, F-67070 Strasbourg Cedex, France

Received January 5, 2006

Dinuclear, divalent acetylacetonato (acac) complexes of the type [M(acac){μ-C_6H_2(⋯NR)$_4$}M(acac)] (M = Ni, Pd) have been prepared by the reaction of the corresponding bis(acac) metal precursor with 2,5-diamino-1,4-benzoquinonediimines $C_6H_2(NHR)_2(=NR)_2$ (**4a**, R = CH_2-*t*-Bu; **4b**, R = CH_2Ph; **4c**, R = Ph), which are metalated and become bridging ligands, also like in the complex [(C_8H_{11})Pt{μ-C_6H_2(⋯NCH_2-*t*-Bu)$_4$}Pt(C_8H_{11})] (**6**) obtained by the reaction of **4a** with [$PtCl_2$(COD)]. The complexes were fully characterized, including by X-ray diffraction for [Ni(acac){μ-C_6H_2(⋯NCH_2Ph)$_4$}Ni(acac)] (**9b**) and [Pd(acac){μ-C_6H_2(⋯NCH_2-*t*-Bu)$_4$}Pd(acac)] (**10a**). The coordination geometry around the metal ions is square-planar, and a complete electronic delocalization of the quinonoid π system occurs between the metal centers over the two N⋯C⋯C⋯C⋯N halves of the ligand. The nature of the N substituent explains the differences between the supramolecular stacking arrangements found for [Ni(acac){μ-C_6H_2(⋯NR)$_4$}Ni(acac)] (**9a**; R = CH_2-*t*-Bu; **9b**, R = CH_2Ph). The Ni complexes were evaluated as catalyst precursors for ethylene oligomerization in the presence of $AlEtCl_2$ or MAO as the cocatalyst, in particular in order to study possible cooperative effects resulting from electronic communication between the metal centers and to examine the influence of the N substituent on the activity and selectivity. These catalysts afforded mostly ethylene dimers and trimers.

Introduction

The field of ethylene polymerization and oligomerization catalysis with late transition metals has witnessed a phenomenal growth over the past 10 years.[1−7] It was triggered by the discovery of highly active Ni^{II} and Pd^{II} precatalysts for ethylene polymerization and oligomerization, which are based on sterically hindered diimine ligands of type **1**.[8] Some catalysts produced oligomers in the range C_6−C_{24} with a

* To whom correspondence should be addressed. E-mail: braunst@chimie.u-strasbg.fr.

(1) For example, see: (a) Heinicke, J.; Peulecke, N.; Köhler, M.; He, M.; Keim, W. *J. Organomet. Chem.* **2005**, *690*, 2449−2457. (b) Nelkenbaum, E.; Kapon, M.; Eisen, M. S. *Organometallics* **2005**, *24*, 2645−2659. (c) Kim, I.; Kwak, C. H.; Kim, J. S.; Ha, C.-S. *Appl. Catal. A* **2005**, *287*, 98−107. (d) Dixon, J. T.; Green, M. J.; Hess, F. M.; Morgan, D. H. *J. Organomet. Chem.* **2004**, *689*, 3641−3668.

(2) *Late Transition Metal Polymerization Catalysis*; Rieger, B., Baugh, L. S., Kacker, S., Striegler, S., Eds.; Wiley-VCH: Weinheim, Germany, 2003.

(3) (a) Britovsek, G. J. P.; Gibson, V. C.; Wass, D. F. *Angew. Chem., Int. Ed.* **1999**, *38*, 428−447. (b) Gibson, V. C.; Spitzmesser, S. K. *Chem. Rev.* **2003**, *103*, 283−315.

(4) Mecking, S. *Coord. Chem. Rev.* **2000**, *203*, 325−351.

(5) Ittel, S. D.; Johnson, L. K.; Brookhart, M. *Chem. Rev.* **2000**, *100*, 1169−1203.

(6) Vogt, D. In *Applied Homogeneous Catalysis with Organometallic Compounds*; Cornils, B., Herrmann, W. A., Eds.; VCH: Weinheim, Germany, 1996; Vol. 1, pp 245−256.

(7) Speiser, F.; Braunstein, P.; Saussine, L. *Acc. Chem. Res.* **2005**, *38*, 784−793 and references cited therein.

(8) (a) Johnson, L. K.; Killian, C. M.; Brookhart, M. *J. Am. Chem. Soc.* **1995**, *117*, 6414−6415. (b) Killian, C. M.; Tempel, D. J.; Johnson, L. K.; Brookhart, M. *J. Am. Chem. Soc.* **1996**, *118*, 11664−11665. (c) Feldman, J.; McLain, S. J.; Parthasarathy, A.; Marshall, W. J.; Calabrese, J. C.; Arthur, S. D. *Organometallics* **1997**, *16*, 1514−1516. (d) Killian, C. M.; Johnson, L. K.; Brookhart, M. *Organometallics* **1997**, *16*, 2005−2007. (e) Mecking, S.; Johnson, L. K.; Wang, L.; Brookhart, M. *J. Am. Chem. Soc.* **1998**, *120*, 888−899.

10.1021/ic060019o CCC: $33.50
Published on Web 05/11/2006

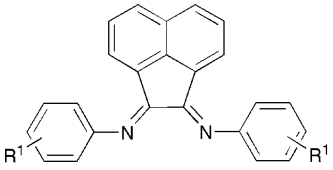

1

R^1 = 2,6-*i*-Pr, 2,6-*t*-Bu

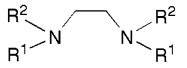

2a R^1 = Et, R^2 = Ph

2b R^1 = H, R^2 = Cy

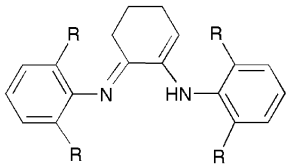

R = Me, *i*-Pr

3a

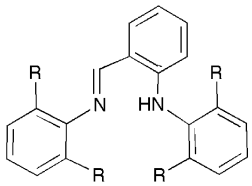

R = Me, *i*-Pr

3b

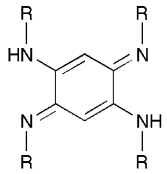

4

selectivity of 94% for α-olefins.[8c] Continuing research efforts have produced other interesting N−N chelating ligands; in particular, bis(amino) ligands **2**[9] and amino−imine ligands **3**,[10,11] which have been successfully applied to olefin polymerization.[3,5]

It is obvious that the design of the organometallic precatalysts, in particular the nature and the architecture of the chelating ligands, is a key point for the control of their reactivity and selectivity. In the course of our studies on the use of functional ligands to design new active catalysts for the oligomerization of ethylene,[12−17] we noticed that the coordination chemistry of 2,5-diamino-1,4-benzoquinonediimine (dabqdiH_2) ligands of type **4** has remained very little explored, despite the presence of two amino−imine chelating sites in the same molecule. Such ligands could be viewed as hybrids between the diamine and diimine type ligands mentioned above. The first use of **4** (R = Ph) as a ligand for the synthesis of metal complexes was only described in 1998 by Kaim and co-workers, who observed a *p*- to *o*-quinone isomerization of azophenine induced by metal coordination and the formation of a cationic mononuclear copper complex.[18] More recently, this group has also reported a related neutral mononuclear Re complex[19] whereas we obtained, at the same time, the mononuclear tetracarbonyl W complexes *cis*-[W(CO)$_4${C_6H_2(NHR)$_2$(=NR)$_2$}] (**5a**, R = CH_2-*t*-Bu; **5b**, R = CH_2Ph) from the corresponding ligands **4a** and **4b**, respectively.[20] In 2000, Lever and co-workers described the synthesis of a dinuclear Ru complex using **4** (R = H), but the product contained an oxidized form of the bridging ligand, which prevented electronic communication between the two metal centers.[21] To the best of our knowledge, only one Pt_2 complex[22] has been prepared by metalation of a ligand of type **4** (molecule **4a** for which R = CH_2-*t*-Bu) with [$PtCl_2$(COD)]. The recent observations that the COD ligand in [$PtCl_2$(COD)] can undergo unusual C−H activation reactions[23] have led us to reexamine its structure in this Pt_2 complex (see below). The X-ray structure of **6** revealed a benzoquinonediimine structure in which the π system is fully delocalized between the metal centers and over the N atoms of the bridging ligand.[22]

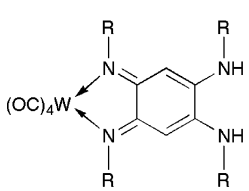

5a R = CH_2*t*-Bu

5b R = CH_2Ph

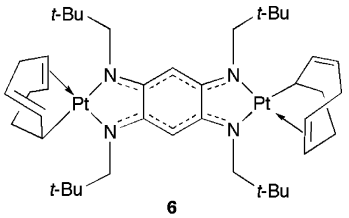

6

This dinuclear complex can be related to homodinuclear oxalamidinato complexes of type **7** recently reported by Walther and co-workers.[24] These authors have shown that only the Ni^{II} complexes bearing terminal acac groups, with their π system fully delocalized between the metal centers, are selective precatalysts for the oligomerization or polymerization of ethylene upon activation with MAO or $AlEt_3$.

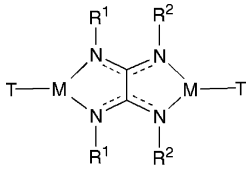

M = Ni, Pd; T = acac, allyl

7

Recent studies with bis-chelating N,O systems of the type 2,5-dioxido-1,4-benzoquinonediimine able to stabilize various

(9) Johnson, L. K.; Feldman, J.; Kreutzer, K. A.; McLain, S. J.; Bennett, A. M. A.; Coughlin, E. B.; Donald, D. S.; Nelson, L. T. J.; Parthasarathy, A.; Shen, X.; Tam, W.; Yang, Y. U.S. Patent 5,714,-556, 1997 (to DuPont).

(10) Ban, K.; Nitabara, M.; Fukuoka, D. Jpn Patent JP 10182679, 1998 (to Mitsui Petrochemical Industries).

(11) Gao, H.; Guo, W.; Bao, F.; Gui, G.; Zhang, J.; Zhu, F.; Wu, Q. *Organometallics* **2004**, *23*, 6273−6280.

(12) Braunstein, P. *J. Organomet. Chem*. **2004**, *689*, 3953−3967.

(13) (a) Braunstein, P.; Chauvin, Y.; Mercier, S.; Saussine, L. *C. R. Chim.* **2005**, *8*, 31−38. (b) Braunstein, P.; Chauvin, Y.; Mercier, S.; Saussine, L.; DeCian, A.; Fischer, J. *J. Chem. Soc., Chem. Commun.* **1994**, 2203−2204.

(14) (a) Speiser, F.; Braunstein, P.; Saussine, L. *Dalton Trans.* **2004**, 1539−1545. (b) Speiser, F.; Braunstein, P.; Saussine, L. *Organometallics* **2004**, *23*, 2633−2640. (c) Speiser, F.; Braunstein, P.; Saussine, L. *Organometallics* **2004**, *23*, 2625−2632. (d) Speiser, F.; Braunstein, P.; Saussine, L.; Welter, R. *Organometallics* **2004**, *23*, 2613−2624.

(15) Speiser, F.; Braunstein, P.; Saussine, L. *Inorg. Chem.* **2004**, *43*, 1649−1658.

(16) Pietsch, J.; Braunstein, P.; Chauvin, Y. *New J. Chem*. **1998**, 467−472.

(17) Braunstein, P.; Pietsch, J.; Chauvin, Y.; Mercier, S.; Saussine, L.; DeCian, A.; Fischer, J. *J. Chem. Soc., Dalton Trans.* **1996**, 3571−3574.

(18) Rall, J.; Stange, A. F.; Hübler, K.; Kaim, W. *Angew. Chem., Int. Ed.* **1998**, *37*, 2681−2682.

(19) Frantz, S.; Rall, J.; Hartenbach, I.; Schleid, T.; Zalis, S.; Kaim, W. *Chem.−Eur. J.* **2004**, *10*, 149−154.

(20) Braunstein, P.; Demessence, A.; Siri, O.; Taquet, J.-p. *C. R. Chim.* **2004**, *7*, 909−913.

(21) Masui, H.; Freda, A. L.; Zerner, M. C.; Lever, A. B. P. *Inorg. Chem* **2000**, *39*, 141−152.

(22) Siri, O.; Braunstein, P. *Chem. Commun.* **2000**, 2223−2224.

Scheme 1. Suggested Mechanism for the Formation of **6**

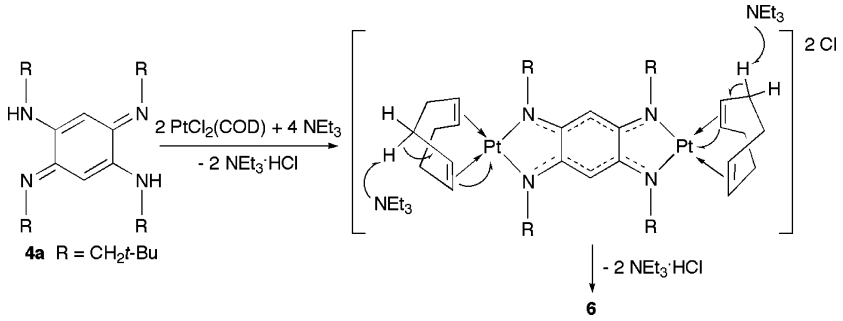

oxidation states of a metal are also worth mentioning in this context.[25] We decided to explore in more detail the coordination properties of dabqdiH_2 ligands of type **4**, which are now readily accessible and whose steric and electronic properties can be fine-tuned.[26,27] We first needed to find general methods for metal complexation and anticipated that dinuclear late-transition-metal complexes, connected via the extended conjugated π system of the ligand, could be attractive candidates for the occurrence of cooperative effects in catalytic reactions, in particular the oligomerization of ethylene, which is a reaction of considerable interest in both academic and industrial sectors.[6,7,28−30] Cooperative effects in catalysis are of great current interest[31−33] and were recently emphasized by the preparation of highly active dinuclear Ni^{II} single-component catalysts for ethylene polymerization containing a 2,5-disubstituted amino-*p*-benzoquinone ligand, as in **8a**,[32] or a 3,3′-bisalicylaldimine ligand, as in **8b**.[33]

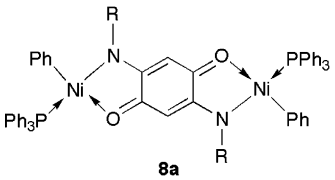

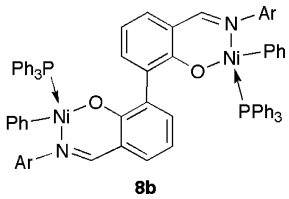

In this paper, we reexamine the structure of the COD-derived moiety in the Pt_2 complex based on **4** and describe the preparation, structural, and dynamic properties of well-defined dinuclear Ni^{II} and Pd^{II} complexes containing dabqdi ligands. The capacity of Ni^{II} complexes to act as precatalysts in the oligomerization of ethylene upon activation with Et_2-AlCl or MAO has also been investigated.

Results and Discussion

Reexamination of the Structure of the Pt_2 Complex 6. In 2000, we described the first dinuclear complex obtained by the metalation reaction of **4a**.[22] It was formed in a basic medium and originally isolated in 15% yield based on its precursor [$PtCl_2$(COD)]. An X-ray analysis showed a crystallographic disorder on the COD-derived moiety, which led to its formulation as a C_8H_{13} ligand, σ,π-bonded to the Pt^{II} center. More recently, unusual base-promoted C−H activation in the α position to the coordinated olefin in the {Pt(COD)} fragment has been reported.[23] This prompted us to reexamine our reaction and improve the synthesis (see the Experimental Section), and we now conclude that the correct formulation for this ligand is C_8H_{11}, as shown in [(C_8H_{11})Pt{μ-C_6H_2(···NCH_2-*t*-Bu)$_4$}Pt(C_8H_{11})] (**6**). This is consistent with mass spectroscopy data (MALDI-TOF) and the observation of the molecular peak at $m/z = 1019.5$ (M + 1). The proposed mechanism for the transformation of the coordinated COD ligand involves the formation of a cationic intermediate from the reaction between [$PtCl_2$(COD)] and ligand **4a** (Scheme 1),[22,26] followed by monodeprotonation of a CH_2 group by NEt_3, leading to a (1,2-η^2-6-σ-cycloocta-1,4-dienyl) ligand, as was recently suggested for a related reaction with a quinolinylamine ligand in the presence of NEt_3.[23a]

Synthesis of Dinuclear Ni^{II} and Pd^{II} Complexes. The dinuclear acetylacetonato (acac) complexes **9** and **10** were obtained in good yields from the reaction between the corresponding bis(acac) metal precursor and the known dabqdiH_2 ligands **4a**−**4c**[22,26,27,34] (Scheme 2).

This method was first applied to the synthesis of Ni^{II} complexes with ligands **4a** and **4c**[35] and is now fully detailed

(23) (a) Peters, J. C.; Harkins, S. B.; Brown, S. D.; Day, M. W. *Inorg. Chem.* **2001**, *40*, 5083−5091. (b) Mas-Ballesté, R.; Champkin, P. A.; Clegg, W.; González-Duarte, P.; Lledós, A.; Ujaque, G. *Organometallics* **2004**, *23*, 2522−2532. (c) Petz, W.; Kutschera, C.; Neumüller, B. *Organometallics* **2005**, *24*, 5038−5043.
(24) (a) Döhler, T.; Görls, H.; Walther, D. *Chem. Commun.* **2000**, 945−946. (b) Walther, D.; Döhler, T.; Theyssen, N.; Görls, H. *Eur. J. Inorg. Chem.* **2001**, 2049−2060. (c) Rau, S.; Lamm, K.; Görls, H.; Schöffel, J.; Walther, D. *J. Organomet. Chem.* **2004**, *689*, 3582−3592.
(25) Kar, S.; Sarkar, B.; Ghumaan, S.; Janardanan, D.; van Slageren, J.; Fiedler, J.; Puranik, V. G.; Sunoj, R. B.; Kaim, W.; Lahiri, G. K. *Chem.—Eur. J.* **2005**, *11*, 4901−4911.
(26) Siri, O.; Braunstein, P.; Rohmer, M.-M.; Bénard, M.; Welter, R. *J. Am. Chem. Soc.* **2003**, *125*, 13793−13803.
(27) Elhabiri, M.; Siri, O.; Sornosa-Tent, A.; Albrecht-Gary, A.-M.; Braunstein, P. *Chem.—Eur. J.* **2004**, *10*, 134−141.
(28) Small, B. L. *Organometallics* **2003**, *22*, 3178−3183.
(29) Chauvin, Y.; Olivier, H. In *Applied Homogeneous Catalysis with Organometallic Compounds*; Cornils, B., Herrmann, W. A., Eds.; VCH: Weinheim, Germany, 1996; Vol. 1, pp 258−268.
(30) Parshall, G. W.; Itell, S. D. *Homogeneous Catalysis: The Applications and Chemistry of Catalysis by Soluble Transition Metal Complexes*; Wiley: New York, 1992.
(31) (a) Tanabiki, M.; Tsuchiya, K.; Motoyama, Y.; Nagashima, H. *Chem. Commun.* **2005**, 3409−3411. (b) Luo, H.-K.; Schumann, H. *J. Mol. Catal. A: Chem.* **2005**, *227*, 153−161. (c) Guo, N.; Li, L.; Marks, T. J. *J. Am. Chem. Soc.* **2004**, *126*, 6542−6543. (d) Li, H.; Li, L.; Marks, T. J.; Liable-Sands, L.; Rheingold, A. L. *J. Am. Chem. Soc.* **2003**, *125*, 10788−10789. (e) Abramo, G. P.; Li, L.; Marks, T. J. *J. Am. Chem. Soc.* **2002**, *124*, 13966−13967.
(32) (a) Zhang, D.; Jin, G.-X. *Organometallics* **2003**, *22*, 2851−2854. (b) Jin, G.-X.; Zhang, D. Chinese Patent CN 1436798, 2003 (to Changchun Applied Chemistry).
(33) Hu, T.; Tang, L.-M.; Li, X.-F.; Li, Y.-S.; Hu, N.-H. *Organometallics* **2005**, *24*, 2628−2632.
(34) Kimish, C. *Ber. Dtsch. Chem. Ges.* **1875**, *8*, 1026.

Scheme 2. Synthesis of the Dinuclear Complexes **9** and **10**

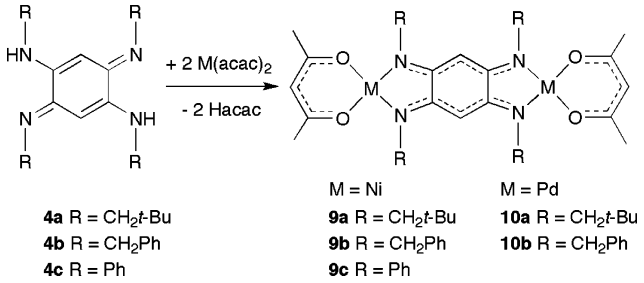

and extended to ligand **4b** and to the synthesis of Pd^{II} complexes. In these reactions, acetylacetone is eliminated and neutral complexes of the type [(acac)M(μ-dabqdi)-M(acac)] **9** and **10** are obtained, in THF at room temperature or in refluxing toluene for 12 h for the Ni complexes and in refluxing toluene for 3 days for the Pd complexes. A slight excess of the dabqdiH_2 ligand was used for the synthesis of the Pd complexes in order to convert all of the Pd precursor, which is more difficult to separate from the reaction mixture than the free ligand.

Complex **10a** could also be prepared in good yield by the reaction between **4a** and 2 equiv of the mononuclear Pd^{II} complex **11**,[36] which also led after ligand redistribution to the formation in ca. 25% yield of the bis(benzoquinonemonoimine)palladium(II) complex **13**[36,37] (Scheme 3).

The formation of these products may be explained by a higher basicity of the quinonic chelate than that of the acetylacetonate chelate and of **4a**. Complex **11** would react first with **4a** to form **10a**, and the eliminated zwitterion **12** would then react with **11** still present in solution to afford **13**, which precipitates in toluene.[36]

The synthesis of [(acac)Zn(dabqdi)Zn(acac)] (**14**) was also attempted starting from [Zn(acac)$_2$], but the product appeared to be unstable in solution, unlike its Ni and Pd analogues.

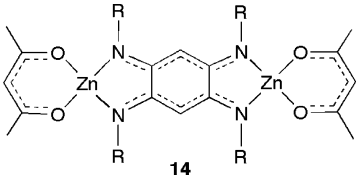

14

In contrast, the reaction of **4a** with [Pt(acac)$_2$] (1.6 equiv of [Pt(acac)$_2$] and 1 equiv of ligand) was unsuccessful owing to the reduced reactivity of the Pt precursor.

The formation of Ni^{II} or Pd^{II} coordination oligomers was not observed in the reactions of Scheme 2, indicating the stability and reduced reactivity of the acac ligands in complexes **9** and **10**, as was also observed in related systems,[24b] which is also confirmed by the lack of reaction between **10a** and zwitterion **12** in THF (in a 1:2 ratio) and between **10a** and 2 equiv of chlorotrimethylsilane in refluxing toluene. Nevertheless, these acac groups do not prevent organoaluminum compounds from forming active catalysts (see below).

Spectroscopic Properties and Crystal Structures. The dinuclear complexes **9** and **10** were characterized by elemental analysis and ^{1}H and ^{13}C{^{1}H} NMR spectroscopic methods, and **10b** was also characterized by mass spectrometry. Both **9b** and **10a** were further characterized by X-ray diffraction. For each compound, the ^{1}H NMR spectrum revealed a structure with the same symmetry as that for the free ligand[22] but with no N−H resonance. Furthermore, the presence of only one signal for each type of proton assigned to the bridging and terminal ligands and the relative integration of all signals clearly proved the centrosymmetry of the molecules.

A fluxional behavior of the NCH_2-*t*-Bu groups of **9a** and **10a** was observed by variable-temperature ^{1}H NMR. The signal of the CH_2 groups appears as a very broad singlet at room temperature and becomes an AB system below coalescence temperature ($^2J_{AB} \approx 8.5$ Hz). For one of the two CH_2 protons, the shape of the signal is that of a multiplet instead of the expected doublet, and this is so far unexplained. The $\Delta G^{\ddagger}$ values calculated for this dynamic behavior are 55.3 and 61 kJ/mol, respectively. This phenomenon, which was not observed with complexes **9b** and **10b** with the less bulky NCH_2Ph substituents, could be explained by steric interactions between these CH_2 protons and the acac group, as was already noticed in related systems,[37] which hinders the free rotation of the neopentyl group around the C−N bond at low temperature.

The N···C···C−H proton of **10a** appears at room temperature as a broad singlet, and the signal for the corresponding H−*C*···C in the ^{13}C{^{1}H} NMR spectrum is broad and weak. This can be improved by increasing the pulse delay to 2 s. Furthermore, a through-space interaction between one CH_2 proton and the N···C···C−H proton was detected by nuclear Overhauser enhancement and further shown by a H−H ROESY experiment at −40 °C.[37]

Green single crystals of complex **9b**, grown from a dichloromethane solution, were used to determine its structure by X-ray analysis (Figure 1). Crystallographic data and selected bond lengths and angles are reported in Tables 1−3. The structure of **9b** consists of a dinuclear centrosymmetric unit in which the dabqdi bridging ligand behaves as a bischelate and bridges two (acac)Ni^{II} fragments. Examination of the bonding parameters within the N1−C2−C1−C3′−N2′ and N2−C3−C1′−C2′−N1′ moieties reveals an equalization of the C−C and C−N bond lengths, which is consistent with a complete electronic delocalization of the π system over these moieties. The C2−C3 and C2′−C3′ bonds, whose length of 1.497(4) Å corresponds to a single bond, connect the two 6π subunits but do not provide conjugation between them.[22] The coordination geometry around the Ni center is square-planar, and in contrast to **9a**,[35] in which the metal centers are slightly out of the plane containing the atoms C1−C3, the 2,5-dibenzylamino-1,4-benzoquinonediimine ligand and the two Ni(acac) fragments are nearly coplanar in **9b** (Figure 2). These geometries lead

(35) Siri, O.; Taquet, J.-p.; Collin, J.-P.; Rohmer, M.-M.; Bénard, M.; Braunstein, P. *Chem.—Eur. J.* **2005**, 11, 7247−7253 and references cited therein.
(36) Braunstein, P.; Siri, O.; Taquet, J.-p.; Rohmer, M.-M.; Bénard, M.; Welter, R. *J. Am. Chem. Soc.* **2003**, *125*, 12246−12256.
(37) Taquet, J.-p.; Siri, O.; Braunstein, P.; Welter, R. *Inorg. Chem.* **2004**, *43*, 6944−6953.

Scheme 3. Alternative Synthesis of **10a**

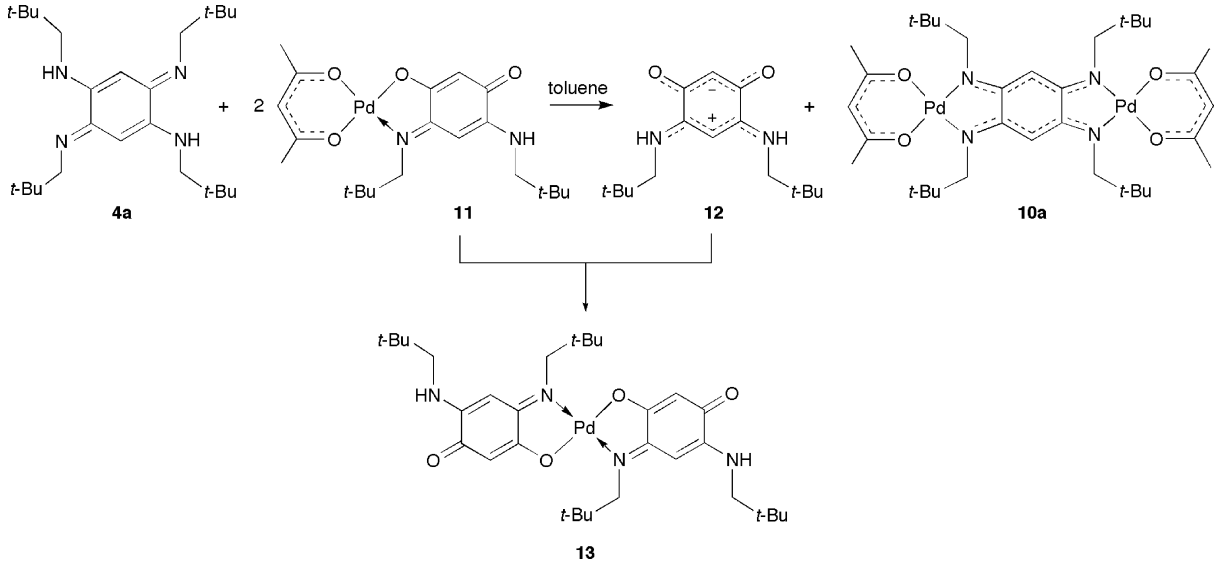

to differences in the stacking arrangements of **9a** and **9b**, imposed by the intermolecular steric crowding generated by the four N substituents. Thus, the distances between the normals to two successive C_6 rings are of 9.09 and 7.68 Å in **9a** and **9b**, respectively. The shorter distance in **9b** results in an intermolecular separation of 3.34 Å between the Ni centers (Figure 2).

The solid-state structure of complex **10a** is shown in Figure 3, and crystallographic data and selected bond lengths and angles are reported in Tables 1−3. This structure is very similar to that of the corresponding Ni_2 complex **9a**.[35] As expected, the coordination geometry around the Pd centers is square-planar. Further comments are not needed for this structure, except the confirmation of the interaction between one CH_2 proton and the N···C···C−H proton, evidenced by a H−H ROESY experiment at −40 °C, with a H···H distance of 2.05(2) Å.

Electronic Spectra. The electronic spectral data are reported in Table 4. In contrast to the UV−vis absorption spectrum of the free ligand **4a**, which shows an intense absorption band at 339 nm corresponding to the $\pi \rightarrow \pi^*$ intraquinone charge transfer,[26] that of the Pt_2 complex **6** revealed two strong absorptions at 479 and 504 nm,[22] with the latter corresponding to a metal-to-ligand charge-transfer (MLCT) transition.

Similarly to the UV−vis absorption spectra of **6**, the dinuclear Ni^{II} complexes are characterized by two strong

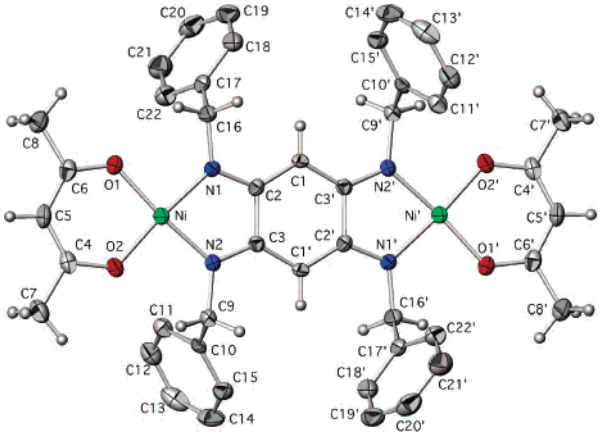

Figure 1. ORTEP view of the Ni_2 complex **9b**. The aryl protons of the benzyl groups have been omitted for clarity. Thermal ellipsoids enclose 50% of the electron density. Operators for generating equivalent, primed atoms: $1 - x, -y, -z$.

Table 1. Crystal Data and Details of the Structure Determination for Compounds **9b** and **10a**

crystal data	**9b**	**10a**
formula	$C_{44}H_{44}N_4O_4Ni_2$	$C_{36}H_{60}N_4O_4Pd_2$
fw [g/mol]	810.25	825.68
cryst syst	triclinic	triclinic
space group	$P\bar{1}$	$P\bar{1}$
a [Å]	8.3480(10)	9.6470(10)
b [Å]	11.403(2)	10.5210(10)
c [Å]	11.905(2)	11.1550(10)
α [deg]	95.18(5)	62.43(5)
β [deg]	110.25(5)	88.13(5)
γ [deg]	111.35(5)	76.50(5)
V [Å^3]	959.5(7)	972.2(6)
Z	1	1
density (calcd) [g/cm^3]	1.402	1.410
μ(Mo Kα) [mm^{-1}]	1.030	0.965
F(000)	424	428
temperature [K]	173	173
θ_{min}, θ_{max} [deg]	1.88, 27.5	2.8, 30.1
data set [h; k; l]	−10/10; −12/14; −15/15	−13/13; −12/14; 0/15
total data, uniq data, R(int)	7808, 4307, 0.053	5676, 5675, 0.000
obsd data [$I > 2\sigma(I)$]	2993	4186
no. of reflns, no. of param	4307, 244	5675, 208
R1, wR2, GOF	0.0644, 0.1263, 1.041	0.0424, 0.0989, 0.792

Table 2. Selected Interatomic Distances (Å) in **9b** and **10a**

	9b	**10a**
C1−C2	1.395(4)	1.413(4)
C1−C3′	1.399(4)	1.401(4)
C2−C3	1.497(4)	1.493(4)
C2−N1	1.326(4)	1.329(4)
C3−N2	1.323(4)	1.332(4)
M−N1	1.874(3)	1.984(2)
M−N2	1.875(3)	1.987(3)
M−O1	1.848(2)	2.009(2)
M−O2	1.846(2)	2.008(2)

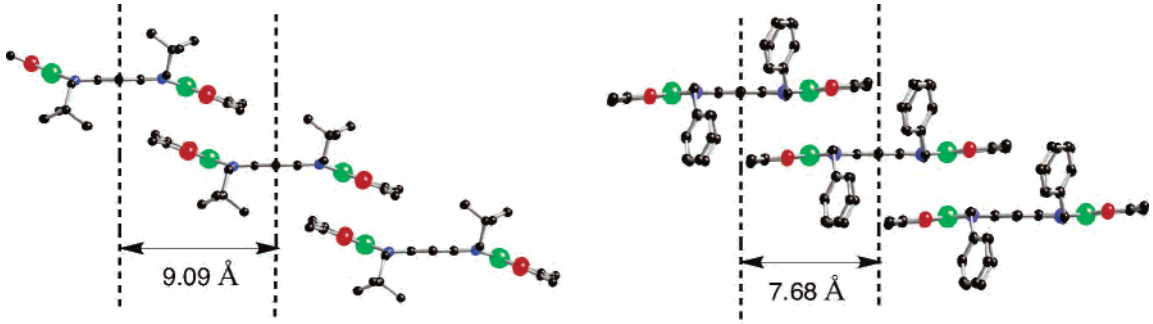

Figure 2. (A) CrystalMaker Views of the stacking arrangements generated in the solid state by **9a** and (B) for comparison by **9b**. Color coding: N, blue; O, red; Ni, green. H atoms have been omitted for clarity.

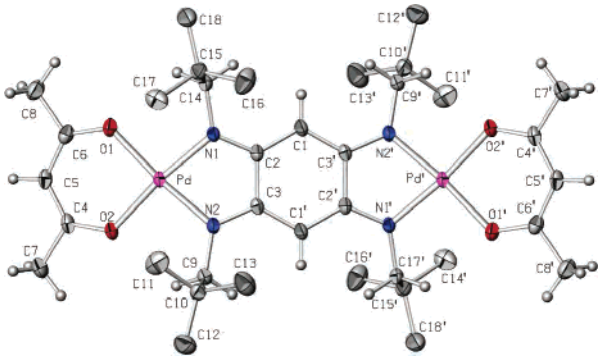

Figure 3. ORTEP view of the Pd_2 complex **10a**. The CH_3 protons of the neopentyl groups have been omitted for clarity. Thermal ellipsoids enclose 50% of the electron density. Operators for generating equivalent, primed atoms: $-x, 1-y, 1-z$.

Table 3. Selected Bond Angles (deg) in **9b** and **10a**

	9b	**10a**
N1−M−N2	83.47(11)	80.14(11)
N1−M−O2	174.21(11)	172.62(9)
N1−M−O1	90.80(11)	94.27(10)
N2−M−O2	91.02(11)	93.40(11)
N2−M−O1	173.68(10)	174.36(9)
O2−M−O1	94.62(10)	92.13(10)

Table 4. Electronic Spectra λ (nm) in CH_2Cl_2

compd	λ (log ϵ)
9a	479 (4.13), 510 (4.17)
9b	486 (4.46), 519 (4.54)
9c	523 (4.22), 555 (4.29)
10a	430 (4.45), 456 (4.64), 491 (4.82)
10b	437 (3.82), 456 (4.00), 488 (4.00)

absorptions in the range 400−600 nm corresponding to a $\pi \rightarrow \pi^*$ intraquinone charge transfer and a MLCT.[35] A significant red shift is observed from **9a** or **9b** to **9c**, which is attributed to an extension of the delocalization of the π system over the Ph substituents on the N atoms (Table 4).

The UV−vis absorption spectra of the dinuclear Pd^{II} complexes **10a** and **10b** are characterized by three strong absorptions at nearly the same wavelengths but with a significant blue shift in comparison to the Ni complexes. The most intense absorption corresponds to a MLCT, and the other two probably correspond to intraquinone charge transfers. There is a difference in the absorption intensities between **10a** and **10b**, which was not the case for **9a** and **9b** (Table 4).

Catalytic Oligomerization of Ethylene. From a general point of view, our dinuclear complexes are interesting candidates for catalytic reactions because they are air-stable, contain readily available ligands, and possess two potentially reactive sites susceptible to showing cooperativity effects. To our knowledge, only a few dinuclear Ni^{II} and Pd^{II} complexes with bridging ligands have been used in ethylene oligomerization and polymerization.[2,24a,b,31−33,38−40] In the neutral dinuclear Ni^{II} complexes of type **15** containing two

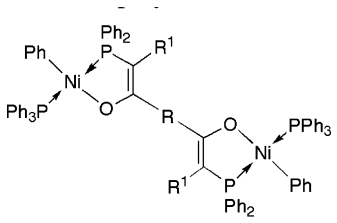

R = aryl, 1,1'-$(\eta^5$-$C_5H_4)_2$Fe
R^1 = H, Ph, Me, SO_3Na

15

(P, O) chelates, a beneficial effect of the conjugation between the active centers separated by a short distance through the spacer ligand R was noticed, which makes these complexes much more active ethylene polymerization catalysts than the mononuclear ones.[40] Furthermore, complexes of type **7**,[24a,b] **8a** with a delocalized π system on the bridging ligand,[32] and **8b**[33] led to higher activities in ethylene oligomerization and/or polymerization.

One of our objectives was to determine whether cooperative effects resulting from electronic communication between the metal centers would lead to improved catalytic activity and/or selectivity, in particular for the production of short-chain oligomers in the presence of only small quantities of cocatalyst. The activity and selectivity of the catalysts were compared to those of $[NiCl_2(PCy_3)_2]$, a typical catalyst for the dimerization of α-olefins.[41] All selectivities reported in

(38) Bianchini, C.; Gonsalvi, L.; Oberhauser, W.; Sémeril, D.; Brüggeller, P.; Gutmann, R. *Dalton Trans.* **2003**, 3869−3875.
(39) (a) Chen, R.; Bacsa, J.; Mapolie, S. F. *Polyhedron* **2003**, *22*, 2855−2861. (b) Chen, R.; Mapolie, S. F. *J. Mol. Catal. A: Chem.* **2003**, *193*, 33−40.
(40) (a) Tomov, A.; Kurtev, K. *J. Mol. Catal. A: Chem.* **1995**, *103*, 95−103. (b) Kurtev, K.; Tomov, A. *J. Mol. Catal.* **1994**, *88*, 141−150.
(41) Commereuc, D.; Chauvin, Y.; Léger, G.; Gaillard, J. *Rev. Institut. Fr. Pét.* **1982**, *37*, 639−649.

Table 5. Influence of the N Substituent and of the Amount of $EtAlCl_2$ Used as the Cocatalyst on the Oligomerization of Ethylene[a]

	9a	**9a**	**9a**	**9b**	**9b**	**9c**	**9c**	$NiCl_2(PCy_3)_2$[7]
$AlEtCl_2$ (equiv)	6	10	14	6	10	6	10	6
selectivity C_4 (mass %)	56	58	57	56	49	58	47	86
selectivity C_6 (mass %)	40	38	40	40	44	36	48	14
selectivity C_8 (mass %)	4	4	3	4	6	6	5	traces
productivity[b]	5000	14500	16500	10500	15000	7000	11000	13000
TOF[c]	10500	30500	34500	22000	31500	14500	23500	27000
linear C_6 (mass %)	52	42	40	49	40	52	35	
α-olefin (C_4) (mol %)	10	5	4	12	2	12	1	9
k_α [d]	0.48	0.4	0.46	0.48	0.6	0.41	0.68	0.13

[a] Conditions: 10 bar of C_2H_4; 35 min; $T = 30$ °C; 4×10^{-2} mmol of the Ni complex; solvent, 15 mL of toluene; [b] Productivity: (g of C_2H_4 consumed)/(g of Ni)·h. [c] TOF: (mol of C_2H_4 consumed)/(mol of Ni)·h. [d] k_α = mol of C_6/mol of C_4.

Table 6. Influence of the N Substituent and of the Amount of MAO Used as the Cocatalyst on the Oligomerization of Ethylene[a]

	9a	**9a**	**9b**	**9b**
MAO (equiv)	100	200	100	200
selectivity C_4 (mass %)	41	46	40	36
selectivity C_6 (mass %)	44	43	47	49
selectivity C_8 (mass %)	15	11	13	14
selectivity C_{10} (mass %)				1
polymer (g)				0.25
productivity[b]	4000	3500	5500	3500
TOF[c]	8500	8000	11000	8000
linear C_6 (mass %)	52	52	50	54
α-olefin (C_4) (mol %)	15	15	12	16
k_α [d]	0.71	0.62	0.77	0.9

[a] Conditions: 10 bar of C_2H_4; 35 min; $T = 30$ °C; 4×10^{-2} mmol of the Ni complex; solvent, 20 mL of toluene; [b] Productivity: (g of C_2H_4 consumed)/(g of Ni)·h. [c] TOF: (mol of C_2H_4 consumed)/(mol of Ni)·h. [d] k_α = mol of C_6/mol of C_4.

the following refer to the total amount of products formed in each catalytic test. In all cases, ethylene pressurization resulted in a rapid exothermic event, indicative of no or very short induction period. The results of the ethylene oligomerization tests for Ni^{II} complexes are reported in Tables 5 and 6. All Pd^{II} complexes were completely inactive in the presence of Et_2AlCl or MAO, consistent with observations made on related systems.[24b]

In general, and despite the presence of two potentially active sites, all catalysts were moderately active compared to $[NiCl_2(PCy_3)_2]$ (Table 5) and completely inactive when less than 6 equiv of $AlEtCl_2$ was added. In general, it also appears that complex **9b** with *N*-benzyl substituents is the most active catalyst precursor, with either $AlEtCl_2$ or MAO as the cocatalyst. Thus, activation with only 6 equiv of $AlEtCl_2$ leads to a turnover frequency (TOF) of 22 000 (mol of C_2H_4)/(mol of Ni)·h for complex **9b**. Increasing the amount of $AlEtCl_2$ to 10 equiv leads to an increased activity of all catalysts. The most spectacular increase was observed for **9a**, from 10 500 to 30 500 (mol of C_2H_4)/(mol of Ni)·h. Only a slight increase of the activity of **9a** was observed when 14 equiv of cocatalyst was used instead of 10 equiv.

The main products were C_4 and C_6 olefins in comparable quantities. Increasing the amount of cocatalyst tends to favor the formation of C_6 oligomers in the case of **9b** and **9c**. Only small quantities of octenes and no long-chain oligomers were observed, which indicates that chain transfer is much faster than chain propagation. Favored by the relatively low pressure of ethylene, the branched fraction of the C_6 oligomers (linear C_6 include 1,5-butadiene, hex-1-ene, hex-2-ene, and hex-3-ene), produced by insertion of butenes in the Ni−C bond of the active species formed after the first ethylene insertion in the catalytic ethylene oligomerization process ($C_4 + C_2$, consecutive reaction), was significant (around 50−65% of the C_6 oligomers). Poor selectivities for 1-butene within the C_4 fraction were observed (maximum of 12%), comparable to $[NiCl_2(PCy_3)_2]$, and an increase in the amount of cocatalyst resulted in a severe decrease of its formation together with a decrease of the linear C_6 fraction. There are no notable differences beween the three complexes in terms of selectivity.

When MAO was used as the cocatalyst in the oligomerization of ethylene, $[NiCl_2(PCy_3)_2]$ decomposed, whereas **9a** and **9b** showed TOFs between 8000 and 11 000 (mol of C_2H_4)/(mol of Ni)·h (Table 5). As for the reactions with $AlEtCl_2$, the main products formed were ethylene dimers and trimers in comparable quantities, except for **9a** with 200 equiv of MAO, where the product distribution was shifted toward the formation of C_6 oligomers and the formation of C_8 oligomers increased to 13%. Small amounts of polymer were only observed with **9b** and 200 equiv of MAO. It thus appears that, although MAO is a less suitable cocatalyst than $AlEtCl_2$ in terms of activity, this leads to a higher selectivity for 1-butene. The k_α values given in Tables 5 and 6 correspond to the molar ratios hexenes/butenes and not to a Schultz−Flory constant. They are larger than those observed recently for Ni^{II} catalyst precursors containing (P, N) chelates.[14]

Conclusion

Dinuclear (acac)Ni^{II} and -Pd^{II} complexes with dabqdi bridges, **9** and **10**, have been prepared in order to examine how metal coordination affects the electronic situation in the $6\pi + 6\pi$ ligand and to evaluate their potential in the catalytic oligomerization of ethylene. The crystal structures of **9b** and **10a** confirmed that in all complexes the geometry of the metal ions is square-planar and a complete electronic delocalization of the quinonoid π system occurs between the metal centers, over the two halves of the ligand. A strong influence of the N substituent in the supramolecular stacking arrangements of **9a** and **9b** was revealed. Whereas the dinuclear Pd^{II} complexes **10a** and **10b** were inactive in the oligomerization of ethylene, the dinuclear Ni^{II} complexes **9a**−**9c** were moderately active in the presence of $AlEtCl_2$, with a maximum TOF of 34 500 (mol of C_2H_4)/(mol of Ni)·h for **9a** activated with 14 equiv of the cocatalyst. Neverthe-

less, they were highly selective for the formation of C_4 and C_6 olefins but with poor selectivities for 1-butene. In the presence of MAO, they were less active but slightly more selective for 1-butene.

This new class of molecules represents one of the rare examples of hybrid amino−imine ligands in which not only their catalytic properties but also their potential as precursors to mixed-valence complexes may be further tuned depending on the nature of the N substituent.[35] Further studies are needed in order to rationalize the effect of the electronic communication between the metal centers on the catalytic activity and/or selectivity and to better understand the influence of the N substituent on the molecular properties, in particular for the preparation of dinuclear complexes with more sterically hindered N substituents that could lead to more selective catalysts and/or for the preparation of dinuclear complexes with different coordination geometries of the metal centers.

Experimental Section

General Procedures. All solvents were dried and distilled using common techniques unless otherwise stated. All manipulations were performed using standard Schlenk techniques under a dry N_2 atmosphere. ^{1}H NMR (300 or 400 MHz) spectra were recorded on a Bruker AC-300 or AMX-400 instrument, and ^{13}C NMR (100 MHz) spectra were recorded on a Bruker AMX-400 instrument. MALDI-TOF mass spectra were recorded on a Biflex III Bruker mass spectrometer. Elemental analyses were performed by the Service de Microanalyses, Université Louis Pasteur (Strasbourg, France). 2,5-Dialkylamino-1,4-benzoquinonediimines **4a** and **4b**, azophenine **4c**, and complexes **9a** and **9c** were prepared according to the literature.[22,26,27,34,35] Gas chromatographic (GC) analyses were performed on a thermoquest GC8000 Top Series gas chromatograph using a Hewlett-Packard PONA column (50-m length, 0.2-mm diameter, and 0.5-mm film thickness). The $\Delta G^{\ddagger}$ values calculated for the dynamic behaviors were calculated with the usual approximation: $\Delta G^{\ddagger} = 4.57T_c(9.97) = \log(T_c/\delta\nu)$.

Improved Synthesis of 6. Ligand **4a** (0.10 g, 0.24 mmol) was dissolved in 100 mL of CH_2Cl_2 in the presence of NEt_3 (2 mL), and solid [$PtCl_2$COD] (0.179 g, 0.48 mmol) was added to the yellow solution. The reaction mixture was stirred overnight at room temperature, and the resulting green solution was evaporated under vacuum. EtOH was then added to the crude product, and insoluble **6** was isolated by filtration and washed with a cold ethanolic solution. Yield: 0.115 g (47%). MS (MALDI-TOF$^+$): *m*/*z* 1019.5 ([M + 1]$^+$). Anal. Calcd for $C_{42}H_{68}N_4Pt_2$: C, 49.50; H, 6.73; N, 5.50. Found: C, 49.75; H, 6.75; N, 5.20.[22]

Synthesis of 9b. Ligand **4b** (0.30 g, 0.60 mmol) was dissolved in 100 mL of THF, and solid [Ni(acac)$_2$] (0.31 g, 1.20 mmol) was added to the yellow solution, which turned rapidly brick red. The reaction mixture was stirred overnight at room temperature, and the resulting red powder of **4b** was filtered, washed with hexane, and dried under vacuum. The filtrate was evaporated and redissolved in dichloromethane. Red crystals suitable for X-ray analysis were obtained by slow evaporation of this solution. Yield: 0.37 g (76%). ^{1}H NMR (300 MHz, $CDCl_3$, 298 K): δ 1.68 (s, 12 H, CH_3 acac), 3.43 (s, 8 H, N−CH_2), 4.60 (s, 2 H, N⋯C⋯C−H), 5.32 (s, 2 H, CH acac), 7.23 (m, 20 H, aryl). ^{13}C{^{1}H} NMR (100 MHz, $CDCl_3$, 298 K): δ 25.58 (CH_3 acac), 47.18 (N−CH_2), 86.77 (H−*C*⋯C⋯N), 101.76 (CH acac), 126.02, 127.34, 128.12 (aryl CH), 140.49 (aryl C), 166.68 (C⋯N), 186.73 (C⋯O). Anal. Calcd for $C_{44}H_{44}N_4O_4Ni_2$: C, 65.22; H, 5.47; N, 6.91. Found: C, 65.15; H, 5.40; N, 6.80.

Synthesis of 10a. Ligand **4a** (0.51 g, 1.23 mmol) and [Pd(acac)$_2$] (0.60 g, 2.00 mmol) were dissolved in 100 mL of toluene, and the resulting solution was heated to reflux for 3 days. The green solution was evaporated at room temperature, and the residue was washed with cold hexane (4 × 100 mL). This powder was then redissolved in 100 mL of dry dichloromethane, and the solution was filtered through Celite and evaporated under vacuum to afford **10a** as a green powder. Green crystals suitable for X-ray analysis were obtained at −30 °C in toluene. Yield: 0.56 g (55%). ^{1}H NMR (400 MHz, $CDCl_3$, 328 K): δ 1.02 (s, 36 H, CH_3), 1.93 (s, 12 H, CH_3 acac), 2.85 (br s, 8 H, N−CH_2), 5.22 (br s, 2 H, N⋯C⋯C−H), 5.30 (s, 2 H, CH acac). ^{1}H NMR (400 MHz, $CDCl_3$, 213 K): δ 1.02 (br s, 36 H, CH_3), 1.93 (br s, 12 H, CH_3 acac), 2.67 (m, $^2J_{HH}$ = 8.4 Hz, 4 H, N−CH*H*), 2.92 (d, $^2J_{HH}$ = 8.4 Hz, 4 H, N−CH*H*), 5.08 (s, 1 H, N⋯C⋯C−H), 5.22 (s, 1 H, N⋯C⋯C−H), 5.32 (s, 1 H, CH acac), 5.33 (s, 1 H, CH acac). ^{13}C{^{1}H} NMR ($CDCl_3$, 298 K): δ 26.60 (CH_3 acac), 29.26 (C*Me*$_3$), 35.50 (br, *C*Me$_3$), 56.17 (N−CH_2), 86.50 (br, H−*C*⋯C⋯N), 100.80 (CH acac), 169.40 (C⋯N), 185.99 (C⋯NO). ^{13}C{^{1}H} NMR (100 MHz, $CDCl_3$, 233 K): δ 27.045 (CH_3 acac), 27.05 (CH_3 acac), 29.18 (C*Me*$_3$), 29.34 (C*Me*$_3$), 34.99 (*C*Me$_3$), 36.23 (*C*Me$_3$), 55.76 (N−CH_2), 55.95 (N−CH_2), 85.78 (H−*C*⋯NC⋯N), 86.88 (H−*C*⋯NC⋯NN), 100.17 (CH acac), 169.09 (C⋯NN), 169.32 (C⋯NN), 186.12 (C⋯NO). The doubling of ^{1}H and ^{13}C{^{1}H} NMR resonances at very low temperature (−60 °C) is so far unexplained. Anal. Calcd for $C_{36}H_{60}N_4O_4Pd_2$: C, 52.36; H, 7.32; N, 6.79. Found: C, 52.75; H, 7.50; N, 6.85.

Synthesis of 10b. Ligand **4b** (0.42 g, 0.96 mmol) and [Pd(acac)$_2$] (0.47 g, 1.54 mmol) were dissolved in 200 mL of toluene, and the resulting solution was heated to reflux for 3 days. The green solution was evaporated at room temperature, and the residue was washed with cold hexane (5 × 100 mL). This powder was redissolved in 100 mL of a 9:1 mixture of dry dichloromethane/toluene, and the solution was filtered through Celite and evaporated under vacuum to afford **10b** as a brown powder. Yield: 0.43 g (49%). ^{1}H NMR (300 MHz, $CDCl_3$, 298 K): δ 1.88 (s, 12 H, CH_3 acac), 4.12 (s, 8 H, N−CH_2), 4.87 (s, 2 H, N⋯C⋯C−H), 5.31 (s, 2 H, CH acac), 7.20 (m, 20 H, aryl), and signals for toluene. The ^{13}C NMR spectrum could not be recorded owing to the poor solubility of **10b**. MS (MALDI-TOF): *m*/*z* 905.955 ([M + 1]$^+$). Anal. Calcd for $C_{44}H_{44}N_4O_4Pd_2 \cdot 0.2C_7H_8$: C, 59.01; H, 4.97; N, 6.06. Found: C, 59.40; H, 4.60; N, 6.10. No better analyses could be obtained for this complex.

Catalytic Oligomerization of Ethylene. All catalytic reactions were carried out in a magnetically stirred (900 rpm) 100-mL stainless steel autoclave, as described in previous papers from this laboratory.[14,15] The interior of the autoclave was protected from corrosion by a protective coating. All catalytic tests were started at 30 °C, and no cooling of the reactor was done during the reaction. After injection of the catalytic solution and of the cocatalyst under a constant low flow of ethylene, the reactor was pressurized to the desired pressure. The temperature increase that was observed resulted solely from the exothermicity of the reaction. The reactor was continuously fed with ethylene by a reserve bottle placed on a balance to allow continuous monitoring of the ethylene uptake. In all of the catalytic experiments, 4×10^{-2} mmol of the Ni complex was used. The oligomerization products and remaining ethylene were only collected from the reactor at the end of the catalytic experiment. At the end of each test, the reactor was cooled to 10 °C before transferring the gaseous phase into a 10-L polyethylene tank filled with water. An aliquot of this gaseous phase

was transferred into a Schlenk flask, previously evacuated for GC analysis. The products in the reactor were hydrolyzed in situ by the addition of ethanol (10 mL), transferred in a Schlenk flask, and separated from the metal complexes by trap-to-trap distillation (120 °C, 20 Torr). All volatiles were evaporated (120 °C, 20 Torr, static pressure) and recovered in a second Schlenk flask previously immersed in liquid N_2 in order to avoid any loss of product. For GC analyses, 1-heptene was used as an internal reference. The required amount of complex was dissolved in 10 mL of chlorobenzene and injected into the reactor. Depending on the amount of cocatalyst added, between 0 and 5 mL of the cocatalyst solution was added so that the total volume of all solutions was 15 mL. When MAO was used as the cocatalyst, the total volume was increased to 20 mL.

Crystal Structure Determination. Diffraction data were collected on a Kappa CCD diffractometer using graphite-monochromated Mo Kα radiation ($\lambda = 0.710\ 73$ Å). The relevant data are summarized in Table 1. Data were collected using ϕ scans, the structures were solved by direct methods using *SHELX97* software,[42,43] and refinement was by full-matrix least squares on F^2. No absorption correction was used. All non-H atoms were refined anisotropically, with H atoms introduced as fixed contributors [d(C−H) = 0.95 Å, $U_{11} = 0.04$]. Full data collection parameters and structural data are available as Supporting Information.

Acknowledgment. We thank the CNRS and the Ministère de la Recherche (Paris) for a Ph.D. grant (J.-p.T.) and the Institut Français du Pétrole for support. We are also grateful to M. Agostinho and M. Mermillon-Fournier for technical assistance.

Supporting Information Available: X-ray data in CIF format. This material is available free of charge via the Internet at http://pubs.acs.org. Crystallographic data for all structures in this paper and a new, corrected CIF file for complex **6** have been deposited with the Cambridge Crystallographic Data Centre, under CCDC 237966, 237967, and 606694, respectively. Copies of this information may be obtained free of charge from The Director, CCDC, 12 Union Road, Cambridge CB2 1EZ, U.K. (fax, +44-1223-336033; e-mail, deposit@ccdc.cam.ac.uk; web, http://www.ccdc.cam.ac.uk).

IC060019O

(42) *Kappa CCD Operation Manual*; Nonius BV: Delft, The Netherlands, 1997.

(43) Sheldrick, G. M. *SHELXL97, Program for the refinement of crystal structures*; University of Gottingen: Gottingen, Germany, 1997.